

DYNAMIC ANALYSIS OF PLATES UNDER MOVING LOADS USING MINDLIN ELEMENTS

Alfredo R. de Faria

Department of Mechanical Engineering, Instituto Tecnológico de Aeronáutica
CTA-ITA-IEM, São José dos Campos, SP 12228-901, Brazil
arfaria@ita.br

Donatus C. D. Oguamanam

Department of Mechanical and Industrial Engineering, Ryerson University,
350 Victoria St., Toronto, ON M5B 2K3, Canada
doguaman@ryerson.ca

Abstract. *The vibration of Mindlin plates with moving concentrated load is investigated using the finite element method (FEM). The use of Mindlin elements may, depending on the refinement of the mesh, yield poor results if the loads are located at off-nodal positions. A new strategy that is based on an adaptive mesh scheme and on the use of perturbation technique in the structural vibration simulation is proposed in this paper to overcome this problem. The strategy supports the use of the traditional finite elements, arbitrary geometry and boundary conditions for both plates and shells.*

Keywords: *moving load, traversing load, adaptive mesh, Mindlin elements, FEM*

1. Introduction

Traversing loads are present in several structural systems, such as bridges, cable railways, railroads, highways cranes and machining tools (Fryba, 1972; Gbadeyan and Oni, 1992; Gbadeyan and Oni, 1995; Huang and Thambiratnam, 2002; Hino *et al.*, 1984). Hence, simulation of moving loads is an important procedure in the design of these systems. However, the investigation of moving loads has been limited to scenarios where beam models provide a reasonable approximation to the system response (Hino *et al.*, 1984, Michaltsos, Sophianopoulos and Kounadis, 1996; Oguamanam, Hansen and Heppler, 1998; Pesterev and Bergman, 1997; Sadiku and Leipholz, 1987; Stanišić, 1985; Stokes, 1849) or to scenarios with simple geometries and boundary conditions such as simply supported rectangular plates (Gbadeyan and Oni, 1992; Gbadeyan and Oni, 1995; Huang and Thambiratnam, 2002; Shadnam, Modif and Akin, 2001). Olsson (1985) presents a general derivation of a FEM application to moving load problems but only reports simulations for beam models.

The few studies addressing plate models work directly with the governing dynamic equations, solving them by an appropriate numerical procedure (e.g. Runge-Kutta) or recurring to schemes that involve separation of variables such as the finite strip method. Regardless of the scheme chosen, trial functions that satisfy very specific boundary conditions must be obtained. However, as soon as the system geometry becomes moderately complex or the boundary conditions diverse, the difficulty in finding such trial functions becomes evident. Moreover, formulations that adopt the classical Kirchoff plate assumptions (zero transverse shear) are often used in FEM based studies of plates under moving loads. This is in sharp contrast with current practice in applied FEM where the use of finite elements that consider transverse shear (Mindlin elements) is prevalent.

This paper is concerned with the appropriateness of Mindlin type elements in modeling plates traversed by concentrated loads. Validation tests show that the accuracy of the results obtained by the FEM when concentrated forces are applied off-nodal positions is poor. Depending on the mesh refinement and boundary conditions imposed the degree of accuracy can be so degenerated that the results in terms of transverse displacements are simply wrong.

Since the concentrated traversing load occupies different positions during the simulation, it is expected that off-nodal loadings will occur. Hence, the lack of accuracy described above will propagate to the dynamic simulations specially because it is highly desirable to use meshes as simple as possible not to burden the computer procedures. An adaptive mesh scheme is employed so as to ensure that the concentrated loads (forces or masses) are always applied at the nodal locations of the elements. Thus the domain is re-meshed at every time-step in order to adjust to the load path. The perturbation technique follows from the observation that while traversing concentrated forces yield constant global matrices those obtained for traversing concentrated masses scenarios are nonconstant because of inertial effects. Thus, modified governing dynamic equations are required and they are solved via the perturbation technique.

2. Problem formulation and governing equations

A schematic of the problem is depicted in Fig. 1. A point mass m moves across the surface of a plate with a prescribed position profile (x_m, y_m) , velocity v_m and acceleration a_m . The thickness of the plate is denoted by the symbol h . The plate is assumed to have arbitrary geometry and boundary conditions.

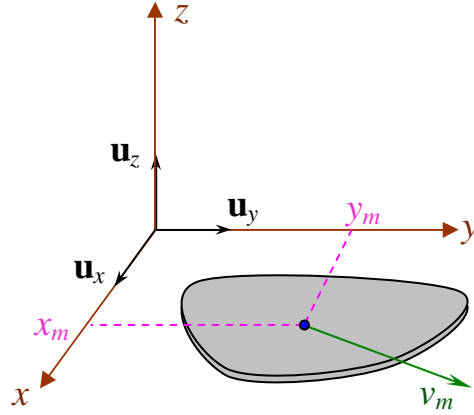


Figure 1. Schematic of a plate with traversing concentrated load

Following the Mindlin plate theory, the in-plane displacement fields \bar{u} and \bar{v} , in the x - and y -axes respectively, are assumed linear in the plate thickness while the transverse displacement \bar{w} is constant through the plate thickness. Thus,

$$\begin{aligned}\bar{u}(x, y, z, t) &= u(x, y, t) + z\psi_x(x, y, t) \\ \bar{v}(x, y, z, t) &= v(x, y, t) + z\psi_y(x, y, t) . \\ \bar{w}(x, y, z, t) &= w(x, y, t)\end{aligned}\quad (1)$$

The linear strain vectors are derived from kinematic relations (1) and they may be written as

$$\boldsymbol{\varepsilon} = \begin{Bmatrix} u_{,x} \\ v_{,y} \\ u_{,y} + v_{,x} \end{Bmatrix} + z \begin{Bmatrix} \psi_{x,x} \\ \psi_{y,y} \\ \psi_{x,y} + \psi_{y,x} \end{Bmatrix} = \boldsymbol{\varepsilon}^0 + z\boldsymbol{\kappa} \quad \boldsymbol{\gamma} = \begin{Bmatrix} w_{,x} + \psi_x \\ w_{,y} + \psi_y \end{Bmatrix} . \quad (2)$$

Given the above strain-displacement relations, the in-plane material stiffness matrix \mathbf{Q} (in-plane) and the transverse shear stiffness \mathbf{Q}_s , the strain energy due to the plate elasticity may be expressed as

$$U_p = \frac{1}{2} \int_{\Omega} \begin{Bmatrix} \boldsymbol{\varepsilon}^0 \\ \boldsymbol{\kappa} \\ \boldsymbol{\gamma} \end{Bmatrix} \begin{bmatrix} \mathbf{A} & \mathbf{B} & \mathbf{0} \\ \mathbf{B} & \mathbf{D} & \mathbf{0} \\ \mathbf{0} & \mathbf{0} & \mathbf{A}_s \end{bmatrix} \begin{Bmatrix} \boldsymbol{\varepsilon}^0 \\ \boldsymbol{\kappa} \\ \boldsymbol{\gamma} \end{Bmatrix} d\Omega , \quad (3)$$

where

$$(\mathbf{A}, \mathbf{B}, \mathbf{D}) = \int_{-h/2}^{h/2} (1, z, z^2) \mathbf{Q} dz \quad \text{and} \quad \mathbf{A}_s = \int_{-h/2}^{h/2} \mathbf{Q}_s dz .$$

If a gravitational field \mathbf{g} is aligned with the plate z axis, the moving mass potential energy W_m and the plate potential energy W_p may be written as

$$W_m = mgw \quad \text{and} \quad W_p = \int_{\Omega} \rho h g w d\Omega . \quad (4)$$

The kinetic energy of the plate is given by

$$T_p = \frac{1}{2} \int_{\Omega} \rho h \left[\dot{u}^2 + \dot{v}^2 + \dot{w}^2 + \frac{h^2}{12} (\dot{\psi}_x^2 + \dot{\psi}_y^2) \right] d\Omega. \quad (5)$$

To derive the kinetic energy of the traversing mass, its position vector \mathbf{r} is given as

$$\mathbf{r} = \left(x + u + \frac{h}{2} \psi_x \right) \mathbf{u}_x + \left(y + v + \frac{h}{2} \psi_y \right) \mathbf{u}_y + w \mathbf{u}_z, \quad (6)$$

where \mathbf{u}_x , \mathbf{u}_y , \mathbf{u}_z are the unit vectors of the xyz reference system. The moving mass kinetic energy can be expressed as

$$T_m = \frac{m}{2} \frac{d\mathbf{r}}{dt} \cdot \frac{d\mathbf{r}}{dt} = \frac{m}{2} \left[\left(\frac{du^*}{dt} \right)^2 + \left(\frac{dv^*}{dt} \right)^2 + \left(\frac{dw}{dt} \right)^2 + 2\dot{x} \frac{du^*}{dt} + 2\dot{y} \frac{dv^*}{dt} + \dot{x}^2 + \dot{y}^2 \right], \quad (7)$$

where $u^* = u + h \psi_x / 2$ and $v^* = v + h \psi_y / 2$. The time derivatives in Eq. (7) are the total derivatives because of convective terms that arise due to the mass movement. The first and second total derivatives are evaluated with the aid of the following:

$$\begin{aligned} \frac{df}{dt} &= \frac{\partial f}{\partial t} + \frac{\partial x}{\partial t} \frac{\partial f}{\partial x} + \frac{\partial y}{\partial t} \frac{\partial f}{\partial y} = \dot{f} + \dot{x} f_{,x} + \dot{y} f_{,y} \\ \frac{d^2 f}{dt^2} &= \ddot{f} + 2\dot{x} \dot{f}_{,x} + 2\dot{y} \dot{f}_{,y} + \ddot{x} f_{,x} + \ddot{y} f_{,y} + \dot{x}^2 f_{,xx} + \dot{y}^2 f_{,yy} + 2\dot{x} \dot{y} f_{,xy} \end{aligned} \quad (8)$$

where f is a dummy function of x , y and t .

The first variation of T_m in Eq. (7) is taken and, integration in time yields, after integration by parts,

$$\int_{t_1}^{t_2} \delta T_m dt = - \int_{t_1}^{t_2} m \left[\frac{d^2 u^*}{dt^2} \delta u^* + \frac{d^2 v^*}{dt^2} \delta v^* + \frac{d^2 w}{dt^2} \delta w + \ddot{x} \delta u^* + \ddot{y} \delta v^* \right] dt. \quad (9)$$

The problem domain is now discretized. The vector of interpolation functions is denoted by the symbol \mathbf{N} and \mathbf{q}_e denotes the vector of elemental nodal variables such that $\mathbf{q}_e = \{ \mathbf{q}_u^T \quad \mathbf{q}_v^T \quad \mathbf{q}_w^T \quad \mathbf{q}_{\psi_x}^T \quad \mathbf{q}_{\psi_y}^T \}^T$. The following definitions are also made:

$$\begin{aligned} u &= [\mathbf{N} \quad \mathbf{0} \quad \mathbf{0} \quad \mathbf{0} \quad \mathbf{0}] \mathbf{q}_e = \mathbf{N}_u \mathbf{q}_e & \psi_x &= [\mathbf{0} \quad \mathbf{0} \quad \mathbf{0} \quad \mathbf{N} \quad \mathbf{0}] \mathbf{q}_e = \mathbf{N}_{\psi_x} \mathbf{q}_e \\ v &= [\mathbf{0} \quad \mathbf{N} \quad \mathbf{0} \quad \mathbf{0} \quad \mathbf{0}] \mathbf{q}_e = \mathbf{N}_v \mathbf{q}_e & \psi_y &= [\mathbf{0} \quad \mathbf{0} \quad \mathbf{0} \quad \mathbf{0} \quad \mathbf{N}] \mathbf{q}_e = \mathbf{N}_{\psi_y} \mathbf{q}_e \\ w &= [\mathbf{0} \quad \mathbf{0} \quad \mathbf{N} \quad \mathbf{0} \quad \mathbf{0}] \mathbf{q}_e = \mathbf{N}_w \mathbf{q}_e & u^* &= [\mathbf{N} \quad \mathbf{0} \quad \mathbf{0} \quad h\mathbf{N}/2 \quad \mathbf{0}] \mathbf{q}_e = \mathbf{N}_{u^*} \mathbf{q}_e \\ & & v^* &= [\mathbf{0} \quad \mathbf{N} \quad \mathbf{0} \quad \mathbf{0} \quad h\mathbf{N}/2] \mathbf{q}_e = \mathbf{N}_{v^*} \mathbf{q}_e \end{aligned} \quad (10)$$

Substitution of terms u , v , w , ψ_x and ψ_y of Eq. (10) in Eqs. (3)-(5) yields the usual element matrices associated with Mindlin elements with a concentrated static mass. The inertia, damping and stiffness matrices and the load vectors which result because of the traversing mass are deduced by substitution for the terms u^* and v^* of Eq. (10) into Eq. (9). These matrices may be written respectively as

$$\begin{aligned} \mathbf{M}_{me} &= m \left(\mathbf{N}_{u^*}^T \mathbf{N}_{u^*} + \mathbf{N}_{v^*}^T \mathbf{N}_{v^*} + \mathbf{N}_w^T \mathbf{N}_w \right) \\ \mathbf{C}_{me} &= 2m \left(\dot{x} \mathbf{N}_{u^*}^T \mathbf{N}_{u^*,x} + \dot{y} \mathbf{N}_{u^*}^T \mathbf{N}_{u^*,y} \right) + 2m \left(\dot{x} \mathbf{N}_{v^*}^T \mathbf{N}_{v^*,x} + \dot{y} \mathbf{N}_{v^*}^T \mathbf{N}_{v^*,y} \right) + 2m \left(\dot{x} \mathbf{N}_w^T \mathbf{N}_{w,x} + \dot{y} \mathbf{N}_w^T \mathbf{N}_{w,y} \right) \\ \mathbf{K}_{me} &= m \left(\ddot{x} \mathbf{N}_{u^*}^T \mathbf{N}_{u^*,x} + \ddot{x} \mathbf{N}_{u^*}^T \mathbf{N}_{u^*,y} + \dot{x}^2 \mathbf{N}_{u^*}^T \mathbf{N}_{u^*,xx} + \dot{y}^2 \mathbf{N}_{u^*}^T \mathbf{N}_{u^*,yy} + 2\dot{x} \dot{y} \mathbf{N}_{u^*}^T \mathbf{N}_{u^*,xy} \right) + \\ & \quad m \left(\ddot{x} \mathbf{N}_{v^*}^T \mathbf{N}_{v^*,x} + \ddot{y} \mathbf{N}_{v^*}^T \mathbf{N}_{v^*,y} + \dot{x}^2 \mathbf{N}_{v^*}^T \mathbf{N}_{v^*,xx} + \dot{y}^2 \mathbf{N}_{v^*}^T \mathbf{N}_{v^*,yy} + 2\dot{x} \dot{y} \mathbf{N}_{v^*}^T \mathbf{N}_{v^*,xy} \right) + \\ & \quad m \left(\ddot{x} \mathbf{N}_w^T \mathbf{N}_{w,x} + \ddot{y} \mathbf{N}_w^T \mathbf{N}_{w,y} + \dot{x}^2 \mathbf{N}_w^T \mathbf{N}_{w,xx} + \dot{y}^2 \mathbf{N}_w^T \mathbf{N}_{w,yy} + 2\dot{x} \dot{y} \mathbf{N}_w^T \mathbf{N}_{w,xy} \right) \\ \mathbf{f}_{me} &= -m \left(\ddot{x} \mathbf{N}_{u^*}^T + \ddot{y} \mathbf{N}_{v^*}^T \right) \end{aligned} \quad (11)$$

The above element matrices are assembled to obtain the system governing dynamic equation which may be expressed as

$$(\mathbf{M} + \mathbf{M}_m)\ddot{\mathbf{q}} + \mathbf{C}_m\dot{\mathbf{q}} + (\mathbf{K} + \mathbf{K}_m)\mathbf{q} = \mathbf{f} + \mathbf{f}_m. \quad (12)$$

This set of equations comprises two types of terms, namely, plate dynamics terms that are independent of x , y , \dot{x} , \dot{y} , \ddot{x} or \ddot{y} (\mathbf{M} , \mathbf{K} and \mathbf{f}) and moving mass contribution terms that are dependent upon x , y , \dot{x} , \dot{y} , \ddot{x} or \ddot{y} (\mathbf{M}_m , \mathbf{C}_m , \mathbf{K}_m and \mathbf{f}_m).

It is plausible to envisage situations where the contributions of the moving loads to the overall system response are negligible when compared with the corresponding terms that are independent of the planar variables x , y and their derivatives. The possibility of these scenarios implies that perturbation based solution techniques can be readily applied to the problem. To this end, the total displacement \mathbf{q} is expanded as a summation of terms,

$$\mathbf{q} = \sum_{i=0}^n \mathbf{q}_i \quad \text{for } n \rightarrow \infty, \text{ such that } \quad \|\mathbf{q}_{i+1}\| < \|\mathbf{q}_i\|. \quad (13)$$

Making use of the above expansion in Eq. (12) permits the decomposition of the system of governing equations into a sequence of equations which may be written as:

$$\begin{aligned} \mathbf{M}\ddot{\mathbf{q}}_0 + \mathbf{K}\mathbf{q}_0 &= \mathbf{f} \\ \mathbf{M}\ddot{\mathbf{q}}_1 + \mathbf{K}\mathbf{q}_1 &= \mathbf{f}_m - \mathbf{M}_m\ddot{\mathbf{q}}_0 - \mathbf{C}_m\dot{\mathbf{q}}_0 - \mathbf{K}_m\mathbf{q}_0 \\ \mathbf{M}\ddot{\mathbf{q}}_2 + \mathbf{K}\mathbf{q}_2 &= -\mathbf{M}_m\ddot{\mathbf{q}}_1 - \mathbf{C}_m\dot{\mathbf{q}}_1 - \mathbf{K}_m\mathbf{q}_1 \\ &\vdots \\ \mathbf{M}\ddot{\mathbf{q}}_n + \mathbf{K}\mathbf{q}_n &= -\mathbf{M}_m\ddot{\mathbf{q}}_{n-1} - \mathbf{C}_m\dot{\mathbf{q}}_{n-1} - \mathbf{K}_m\mathbf{q}_{n-1} \end{aligned} \quad (14)$$

The convergence characteristics of the perturbation series given in Eq. (13) is investigated with a modified form of the governing equation Eq. (12). This is expressed as

$$(\bar{\mathbf{K}} + \bar{\mathbf{K}}_m)\mathbf{q} = \bar{\mathbf{f}} + \bar{\mathbf{f}}_m, \quad (15)$$

where $\bar{\mathbf{K}}$ and $\bar{\mathbf{K}}_m$ represent effective stiffness matrices, and $\bar{\mathbf{f}}$ and $\bar{\mathbf{f}}_m$ denote effective vectors that are typical of forward time integration schemes such as Wilson- θ or Newmark method. The exact solution of the governing equation, Eq. (15), is given as

$$\mathbf{q}_{\text{exact}} = (\mathbf{I} + \bar{\mathbf{K}}^{-1}\bar{\mathbf{K}}_m)^{-1} \bar{\mathbf{K}}^{-1} (\bar{\mathbf{f}} + \bar{\mathbf{f}}_m). \quad (16)$$

For a series expansion with $n + 1$ terms, where $n > 1$, the solutions to the perturbed equations, i.e. Eq. (14), are:

$$\begin{aligned} \mathbf{q}_0 &= \bar{\mathbf{K}}^{-1}\bar{\mathbf{f}} \\ \mathbf{q}_1 &= \bar{\mathbf{K}}^{-1}(\bar{\mathbf{f}}_m - \bar{\mathbf{K}}_m\mathbf{q}_0) \\ \mathbf{q}_2 &= -\bar{\mathbf{K}}^{-1}\bar{\mathbf{K}}_m\mathbf{q}_1 \\ &\vdots \\ \mathbf{q}_n &= -\bar{\mathbf{K}}^{-1}\bar{\mathbf{K}}_m\mathbf{q}_{n-1} \end{aligned} \quad (17)$$

The error \mathbf{e} (i.e. $\sum_i \mathbf{q}_i - \mathbf{q}_{\text{exact}}$) is expanded as

$$\begin{aligned} \mathbf{e} &= \mathbf{q}_0 + (\mathbf{I} + \bar{\mathbf{K}}^{-1}\bar{\mathbf{K}}_m)^{-1} [\mathbf{I} + (-\bar{\mathbf{K}}^{-1}\bar{\mathbf{K}}_m)^n] \bar{\mathbf{K}}^{-1} (\bar{\mathbf{f}}_m - \bar{\mathbf{K}}_m\mathbf{q}_0) - (\mathbf{I} + \bar{\mathbf{K}}^{-1}\bar{\mathbf{K}}_m)^{-1} \bar{\mathbf{K}}^{-1} (\bar{\mathbf{f}} + \bar{\mathbf{f}}_m) = \\ &= (\mathbf{I} + \bar{\mathbf{K}}^{-1}\bar{\mathbf{K}}_m)^{-1} (-\bar{\mathbf{K}}^{-1}\bar{\mathbf{K}}_m)^n \bar{\mathbf{K}}^{-1} (\bar{\mathbf{f}}_m - \bar{\mathbf{K}}_m\bar{\mathbf{K}}^{-1}\bar{\mathbf{f}}) \end{aligned} \quad (18)$$

This shows that the leading term in the error equation is $(\bar{\mathbf{K}}^{-1}\bar{\mathbf{K}}_m)$. If the effects of $\bar{\mathbf{K}}_m$ are very small when compared to those due to $\bar{\mathbf{K}}$, then $(\bar{\mathbf{K}}^{-1}\bar{\mathbf{K}}_m)^n$ must converge to $\mathbf{0}$ as $n \rightarrow \infty$. It is observed via numerical simulations that numerical convergence within machine precision is guaranteed with a small n .

3. Mindlin elements and adaptive meshes

The shear locking (Hughes, 1987) phenomenon associated with Mindlin elements has received a considerable attention in the literature. On the other hand, little or no attention has been directed to the propensity of Mindlin elements to inaccurately predict responses of systems with concentrated loads that are arbitrarily located in the domain of the systems. This may partly be because most of the analyses involving concentrated loads consider such loads to be fixed at a point (i.e. stationary) that is usually coincident with a node.

This observation is demonstrated by the use of a rectangular plate of length 60 m, width 30 m, and thickness of 0.577 m. The plate is clamped along the edges and it is made from a material with a Young's modulus of 200 GPa and a Poisson ratio of 0.30. It is assumed that 100 static load cases are applied on the plate at evenly spaced intervals along the center line lengthwise (i.e. $y = 15$ m). The commercial FEM software Nastran is used to simulate the scenario with bilinear elements CQUAD4.

The first simulation comprises 20 elements along the length and 12 elements along the width. The second has 40 and 24 elements, respectively. Bilinear interpolation functions are used to derive consistent nodal loads at instances when a concentrated load is located at an off-nodal point. The results are depicted in Fig. 2 in terms of normalized displacements.

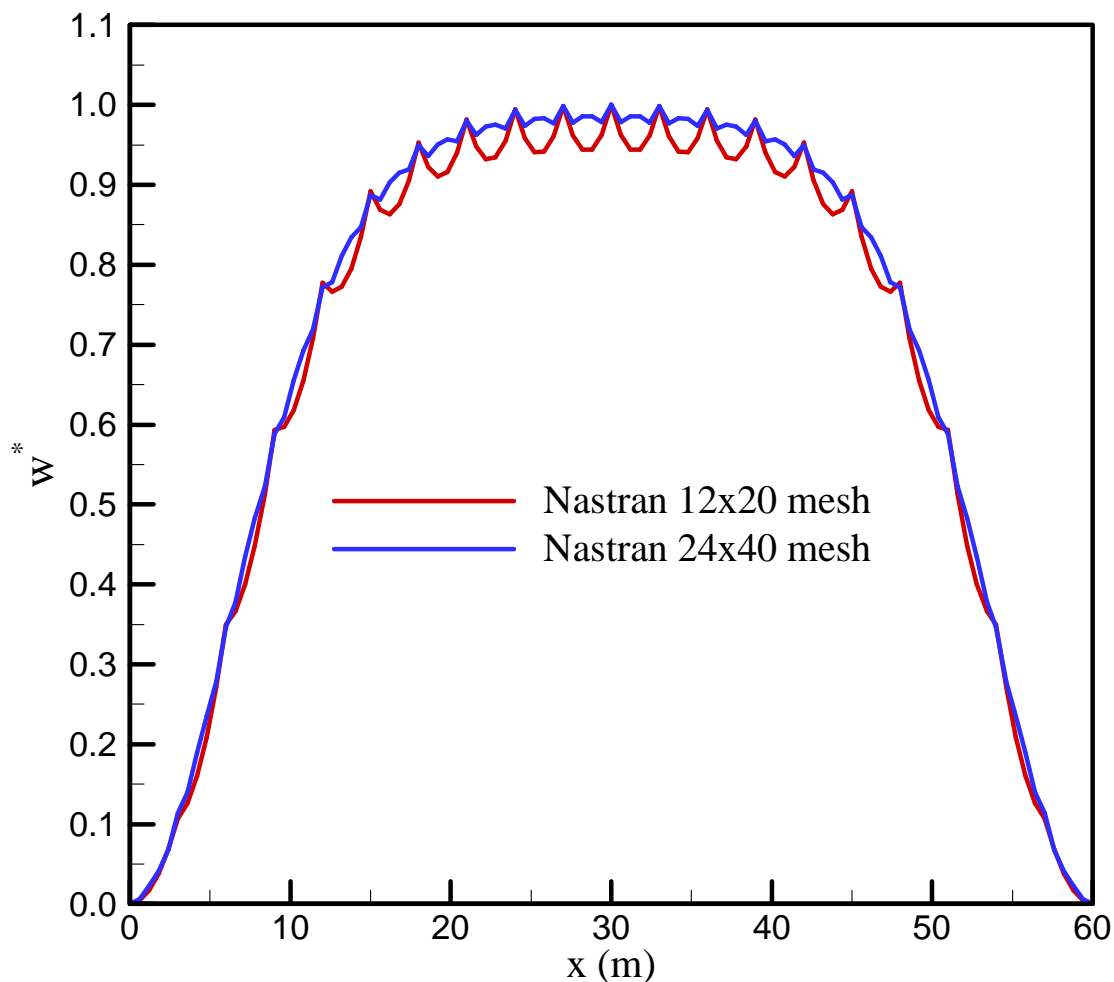


Figure 2. Displacement under stationary load (Nastran results)

The results for an identical scenario but with the use of the adaptive meshing scheme to ensure that the concentrated loads are always at nodal points are shown in Fig. 3. Here a different mesh is generated for each load case. The meshes used to generate these results do not yield the same number of elements but they yield approximately the same number of degrees of freedom. Figure 4 is a schematic of how these elements are distributed in a simple adaptive mesh for three concentrated load locations.

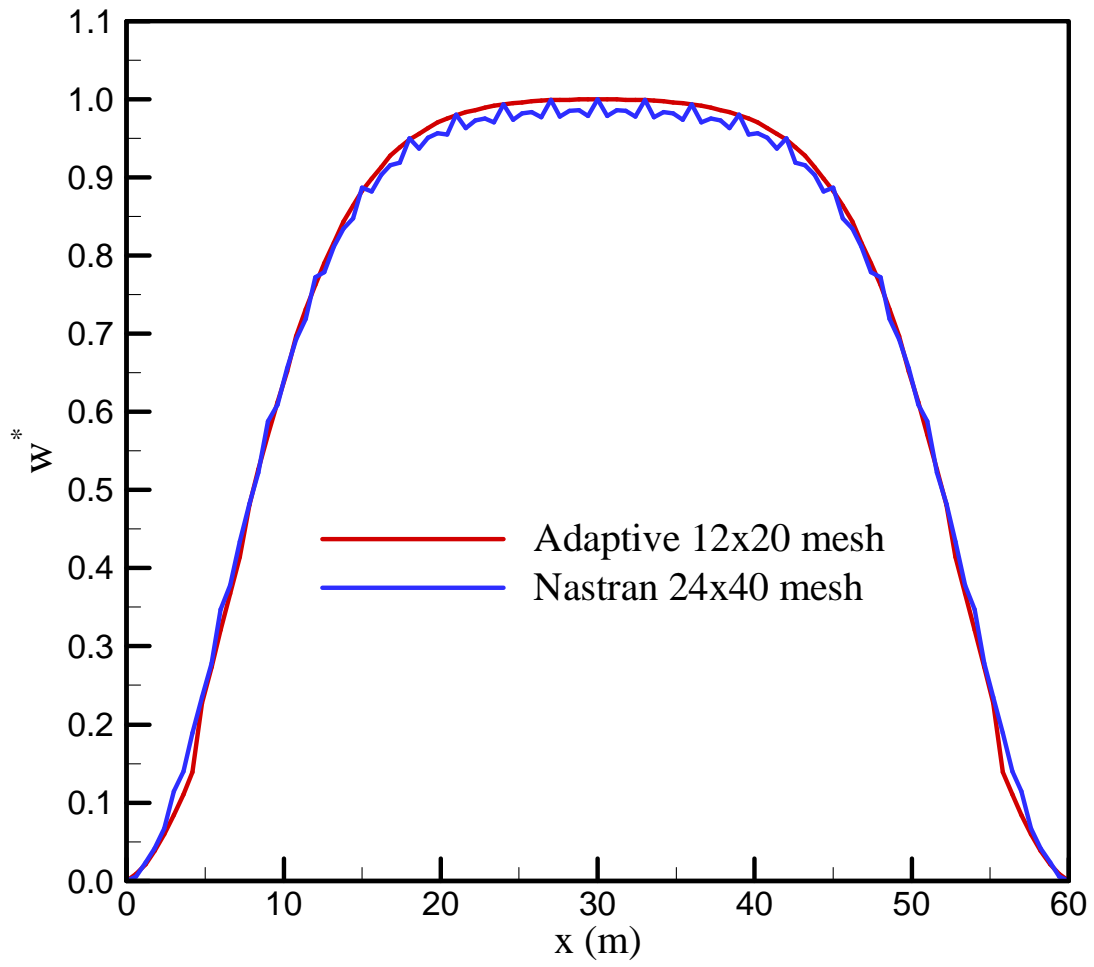


Figure 3. Displacement under stationary load (Nastran fixed and proposed adaptive mesh)

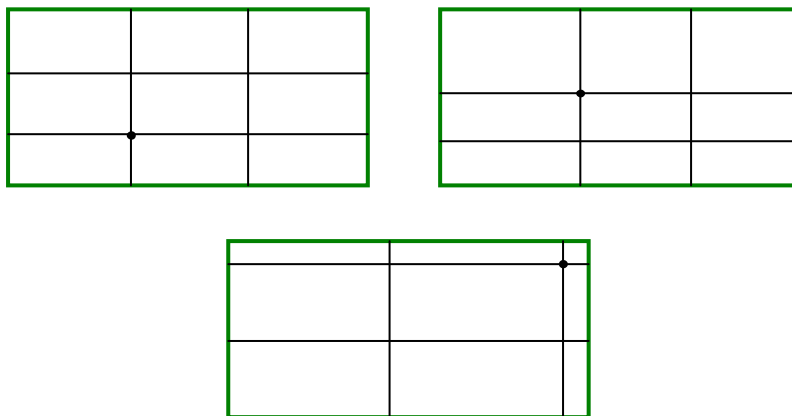


Figure 4. Illustration of the adaptive meshes concept

Given that the mesh in the dynamic problem changes at each time step, it is imperative to develop a procedure to map the old mesh onto the new mesh. Such a procedure can be explained with the aid of Fig. 5. Assume that the degrees of freedom u, v, w, ψ_x, ψ_y associated with node i_{new} of the new mesh are sought. The first step is to identify the element of the old mesh that contains the node i_{new} . The local coordinates ξ, η of node i_{new} are determined thereafter. Finally, the degrees of freedom associated with i_{new} are evaluated and degrees of freedom associated with nodes $i_{\text{old}}, j_{\text{old}}, k_{\text{old}}$ and l_{old} are interpolated using the local coordinates ξ, η that were determined in the second step of the procedure.

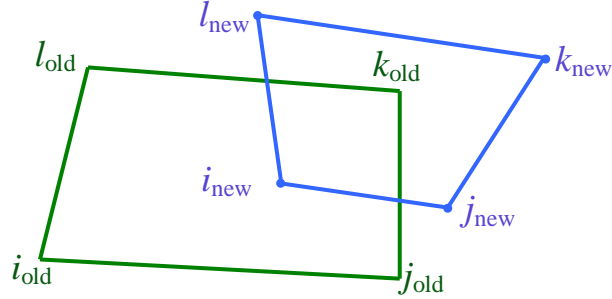


Figure 5. Mesh mapping technique

4. Numerical Simulations

The proposed strategy is independent of the type of structure (i.e. plate or shell), the shape of the structure and the prevailing boundary conditions. For the purpose of demonstration, consider a rectangular plate with a length of 100 m, width of 10 m, and thickness of 0.30 m. The Young's modulus of the material of which the plate is made is 31 GPa, the Poisson ratio is 0.25, and density is 2500 Kg/m³. The plate is simply supported along the two shorter edges and free along the two longer edges.

Two dynamic cases are considered: (i) a concentrated force of 1.0×10^5 N that moves lengthwise with a velocity of 20 m/s, and (ii) a 10,193.68 kg concentrated mass that moves lengthwise with a velocity of 20 m/s. The magnitude of the moving mass is consistent with a gravitational acceleration of 9.81 m/s². The adaptive meshes used comprise two biquadratic elements along the shorter side and twenty biquadratic elements along the longer side.

The overall normalized transverse displacement for both the concentrated force and moving mass are shown in Fig. 6. The normalizing factor is the midpoint transverse displacement of the plate under a concentrated force of 1.0×10^5 N applied transversely at the plate midpoint or center. The magnitude of the displacement in this case is 0.783 m. The results, as depicted in Fig. 6, show that the transverse displacements due to the moving mass are higher than those of the moving force. This observation is in accord with that reported in the literature (Huang and Thambiratnam, 2002; Shadnam, Modif and Akin, 2001); it is solely the consequence of the inertia contributions of the moving mass. Further, it is noted that the ripples in the scenarios without adaptive mesh strategy (i.e. Figs. 2 and 3) are absent.

The perturbation series is as defined in Eq. (13) but with only three terms ($\mathbf{q}_0, \mathbf{q}_1, \mathbf{q}_2$). The contribution of each term to the overall transverse displacement of the plate is initially investigated. A plot of the respective normalized transverse displacements (i.e. w_0^*, w_1^* and w_2^*) is shown in Fig. 7. Also shown is the resulting plate normalized transverse displacement: $w^* = w_0^* + w_1^* + w_2^*$. The plots show that w_0^* is the dominant term. The w_2^* contribution is not noticeable within the scale of the plot. Thus a two-term perturbation series is sufficient for the required precision.

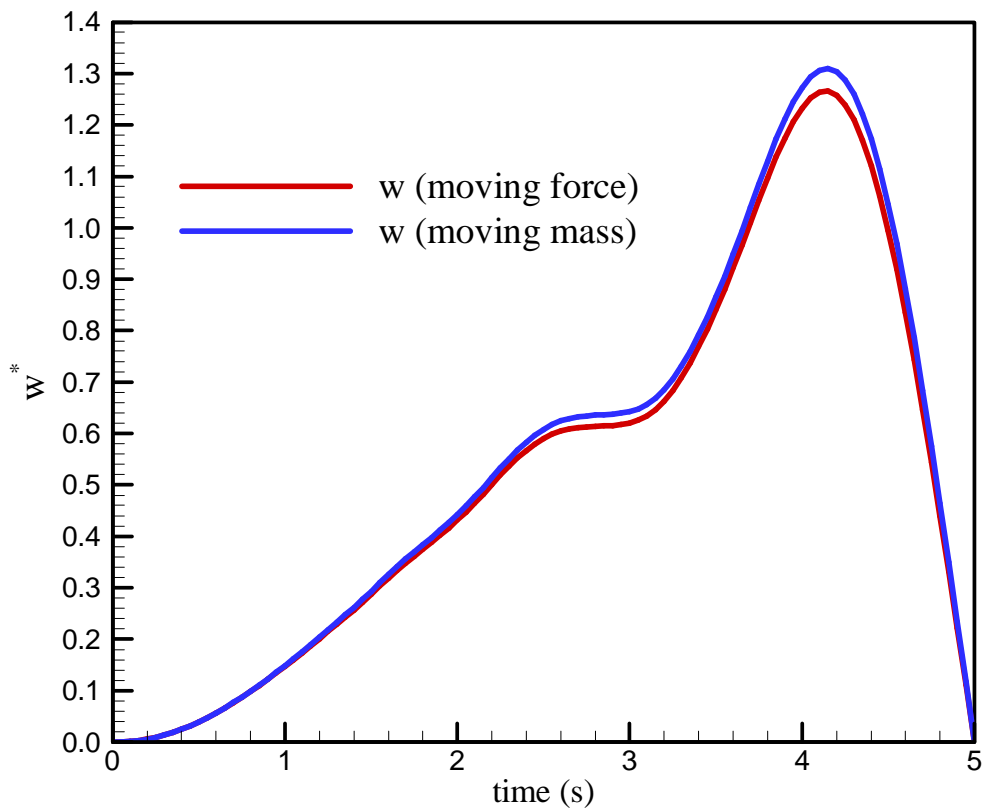


Figure 6. Rectangular plate transverse displacements

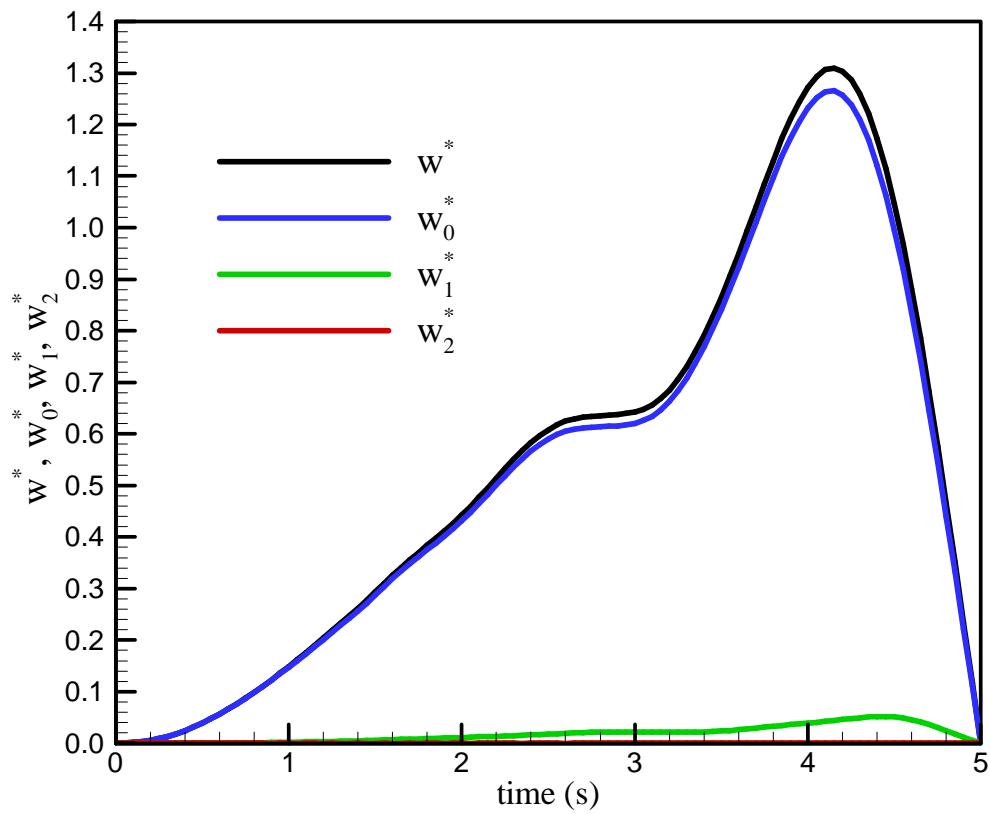


Figure 7. Moving mass transverse displacement contributions

The suitability of the proposed strategy for diverse domain shapes and boundary conditions is now demonstrated via the use of a circular plate that is fully clamped along its perimeter. The plate has 5 m radius, 0.10 m thickness and is made of the same material as that of the rectangular plate in the preceding example. A concentrated load of 1.0×10^3 N orbits around the plate center at a distance of 2 m and with a constant angular velocity of $\pi/10$ rd/s. The meshes used have three biquadratic elements along the radial direction and six biquadratic elements along the circumferential direction.

The result of the simulation is presented in Fig. 8. The dynamic transverse displacements at the plate center are normalized with respect to the transverse displacements at the plate center (0.180 mm) when the concentrated load is applied at the center. The initial state of the system is such that the plate is at rest and the concentrated load is statically positioned at the distance of 2 m from the plate center. This explains the nonzero value ($w^* = 0.53$ to be precise) observed at time $t = 0$ s.

High frequency content is observed in the dynamic response of the circular plate. This constitutes a major complication in the traditional modal decomposition based analysis methods because of the need to include several modes in the analysis. In order to capture the high frequency contributions, the present simulation uses a time step of 0.001 s, which is 50 times smaller than the 0.05 s used in the case of the rectangular plate simulation.

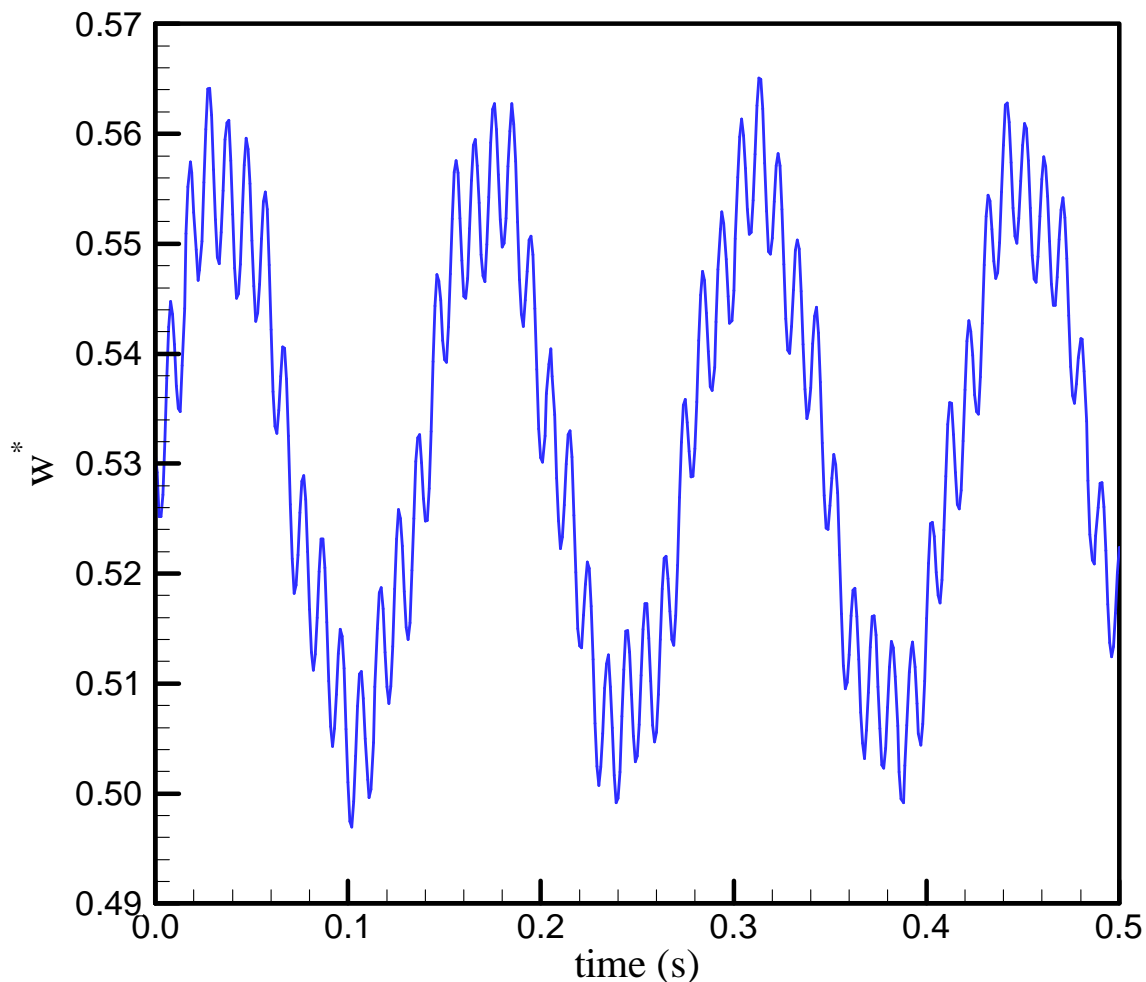


Figure 8. Circular plate transverse displacements

5. Comments and conclusions

The present work proposes a new strategy for the dynamic simulations of concentrated moving loads when relatively coarse meshes are used. The strategy involves the use of adaptive meshes that follow the load path in a manner that ensures that the point of application of the load is always coincident with a node. The adaptivity of the mesh requires the implementation of global matrix decomposition at each time step. This is not computationally prohibitive because of the coarseness of the mesh.

The elements considered in the present study do not experience shear locking and reduced integration is not employed. While this will not be the case when using extremely thin plates, neither the efficacy of the adaptive mesh strategy nor that of the proposed perturbation approach is expected to deteriorate.

The perturbation approach has the advantage of clearly separating the effects of just a concentrated force from those due to inertia consideration. It is observed that the number of terms in the expansion series required for high degree of precision is directly dependent upon the relative inertia between the base structure and the moving mass. Hence scenarios in which heavy masses traverse relatively light base structures would require higher number of terms in the perturbation series and perhaps the use of a nonlinear solver.

6. Acknowledgements

This work was partially financed by the Brazilian agency CNPq (grant 304642/2003-7).

7. References

- Fryba L., 1972, *Vibrations of Solids and Structures under Moving Loads*, Groningen: Noordhoff.
- Gbadeyan, A. and Oni, S.T., 1992, Dynamic response to moving concentrated masses of elastic plates on a non-Winkler elastic foundation, *Journal of Sound and Vibration*, Vol. 154, pp. 343-358.
- Gbadeyan, A. and Oni, S.T., 1995, Dynamic behaviour of beams and rectangular plates under moving loads, *Journal of Sound and Vibration*, Vol. 182, pp. 677-695.
- Hino, J., Yoshimura T., Konishi K. and Ananthanarayana N., 1984, A finite element method prediction of the vibration of a bridge subjected to a moving vehicle load, *Journal of Sound and Vibration*, Vol. 96, pp. 45-53.
- Huang, M.-H. and Thambiratnam, D.P., 2002, Dynamic response of plates on elastic foundation to moving loads, *Journal of Engineering Mechanics*, Vol. 128, pp. 1016-1022.
- Hughes, T.J.R., 1987, *The Finite Element Method*, New Jersey: Prentice-Hall.
- Michaltsos, G., Sophianopoulos, D. and Kounadis, N., 1996, The effect of a moving mass and other parameters on the dynamic response of a simple supported beam, *Journal of Sound and Vibration*, Vol. 191, pp. 357-362.
- Oguamanam, D.C.D., Hansen, J.S. and Heppler, G.R., 1998, Dynamic response of an overhead crane system, *Journal of Sound and Vibration*, Vol. 213, pp. 889-906.
- Oguamanam, D.C.D., Hansen, J.S. and Heppler, G.R., 2001, Dynamics of a three-dimensional overhead crane system, *Journal of Sound and Vibration*, Vol. 242, pp. 411-426.
- Olsson, M., 1985, Finite element, modal co-ordinate analysis of structures subjected to moving loads, *Journal of Sound and Vibration*, Vol. 99, pp. 1-12.
- Pesterev, A.V. and Bergman, L.A., 1997, Response of elastic continuum carrying moving linear oscillator, *Journal of Engineering Mechanics*, Vol. 123, pp. 878-884.
- Sadiku, S. and Leipholz, H.H.E., 1987, On the dynamics of elastic systems with moving concentrated masses, *Ingenieur-Archives*, Vol. 57, pp. 223-242.
- Shadnam, M.R., Modif, M. and Akin, J.E., 2001, On the dynamic response of rectangular plate with moving mass, *Thin-Walled Structures*, Vol. 39, pp. 797-806.
- Stanišić, M.M., 1985, On a new theory of the dynamic behaviour of the structures carrying moving masses, *Ingenieur-Archives*, Vol. 55, pp. 176-185.
- Stokes, G.G., 1849, Discussion of a differential equation relating to the breaking of railway bridges, *Transactions of the Cambridge Philosophic Society*, Vol. 5, pp. 707-735.

8. Responsibility notice

The authors are the only responsible for the printed material included in this paper.